

AIRWORTHINESS INVESTIGATION OF A HIGHLY NONPLANAR FLEXIBLE WING CONCEPT

Klaus Seywald* , Fabian Hellmundt* , Andreas Wildschek* , Florian Holzapfel**
***Airbus Group Innovations, **TUM Institute of Flight System Dynamics**

Keywords: *aeroelasticity, flight dynamics, nonplanar wing, flutter*

Abstract

An Airbus Group Innovations toolchain being developed for the airworthiness assessment of innovative aircraft configurations in the early design stage was applied and tested on a highly non-planar flexible wing concept, the C-wing. The toolchain is incorporating the steady and unsteady vortex lattice method coupled to a non-linear beam model featuring automated preliminary structural sizing and weight estimation. A coupled flight dynamic aeroelastic flight simulation model is generated enabling both a fast and a real time simulation of the investigated configuration. A number of EASA CS-25 requirements are checked and assessed pointing out problems to be expected and assessing the feasibility of the concept with respect to aeroelasticity and flight dynamics.

1 Introduction

The demand for improving the fuel efficiency of transport aircraft leads towards unconventional designs. High potential for efficiency improvement was found in nonplanar wings, promising a significant reduction of induced drag [1]. Another trend observed is the increase of structural flexibility, resulting from lighter structures and the potential for aeroelastic tailoring, allowing the adaption of the wing shape for different flight phases. Given these trends the influence of aeroelasticity is becoming an essential feature to be considered in the conceptual design phase in order to unveil problems not covered by classical methods such as [2] or [3]. Flexibility can pose a

significant challenge in aircraft certification, due to the impact on aircraft handling qualities, controllability and performance. The consideration of certification requirements in the early aircraft design enables a more reliable assessment of concept feasibility.

1.1 The C-Wing

A C-shaped wingtip can be exploited to unify several advantages. It was shown that the theoretical induced drag reduction is close to the achievable optimum which can be obtained by a closed biplane, at the same time not increasing the wingspan [1]. This is a significant advantage considering airport parking size limitations. The predicted induced drag reductions are based on potential flow theory investigations but have been shown to hold for high fidelity Euler computations as well [4]. Transport aircraft designs involving a C-wing were shown in [5] and [6] suggesting to replace the horizontal stabilizer by using the top wing for pitch trimming and control. This is further investigated in [7] and [8] showing that trimming is possible for high altitude and high speed cases. Other multidisciplinary investigations of C-shaped wingtips were also made in [9] and [10], however not considering the possibility of pitch trimming and control. Overall benefits considering multidisciplinary aspects of the C-wing were also predicted in [11].

1.2 Integrated Aeroelasticity, Flight Dynamics and Control

The coupling of flight dynamics and aeroelasticity was studied for more than five decades [12]

and is still an important topic of current research. The standard approach established for flight simulation is the mean-axis approach [13]. Shortcomings of the mean-axis approach were noted by various authors such as [14] or [15] and alternative approaches are suggested. Especially for large nonlinear structural deformations, fully coupled aeroelastic flight dynamic models are used such as in [16].

1.3 Aeroelasticity and Certification Requirements in the Design Loop

A common problem in the preliminary assessment of innovative designs is that often only a limited range of the flight envelope is investigated, however for certification of an aircraft it has to comply with the complete set of EASA CS-25 certification requirements [17] over the entire flight envelope. The problem of flying qualities consideration in the early design has been addressed by [18] who has integrated longitudinal flying quality requirements in the multidisciplinary design optimization (MDO) loop for the rigid aircraft. Caja [19] investigated the flight dynamics for a non planar wing in conceptual design limited to the rigid aircraft. Bhasin [20] made nonlinear aeroelastic investigations for the joined wing configuration. The combination of aeroelasticity and longitudinal handling qualities was addressed by [21].

1.4 Outline

This paper addresses the overall aircraft preliminary concept evaluation extending the state of the art depth of assessment by enabling flight simulation considering aeroelastic effects and evaluating EASA CS-25 certification requirements. This allows trim, stability, controllability and handling qualities investigation over the entire flight envelope considering nonlinear dynamic aeroelasticity. An Airbus Group Innovations toolchain established for the preliminary assessment of new aircraft designs is applied to evaluate the described configuration with respect to airworthiness and practical feasibility. A redesign is suggested after showing feasibility issues of the initial design. A rough workflow of the toolchain is

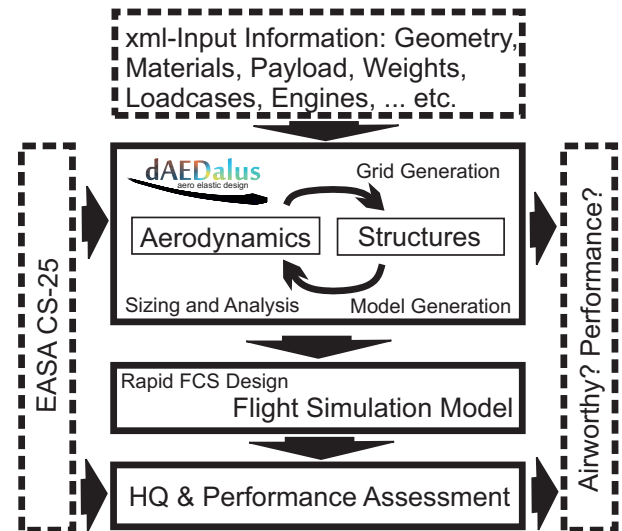


Fig. 1 Toolchain for Airworthiness Assessment

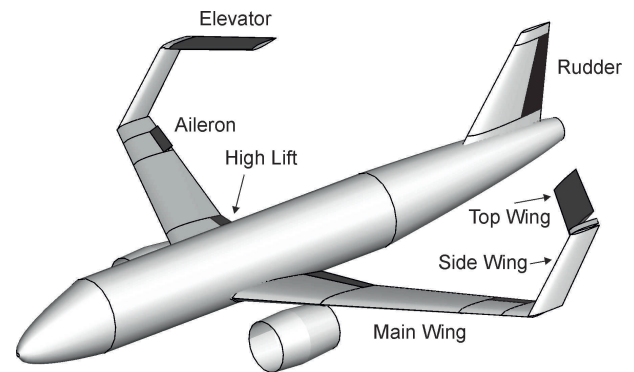


Fig. 2 Concept 1 Geometry

depicted in Figure 1.

2 Modeling

The following investigation is based on the C-wing concept shown in Figure 2. The design is a short to mid range aircraft allowing a maximum payload of 20t. Comparing to a classical configuration the horizontal stabilizer was removed, instead the top wing is applied for pitch control. It is assumed that all control surfaces can deflect by $\pm 25deg$ assuming attached flow under all conditions.

2.1 Aerodynamic Model

The aircraft aerodynamics are modeled by means of potential flow theory. Steady aerodynamic coefficients are computed using a vortex lattice

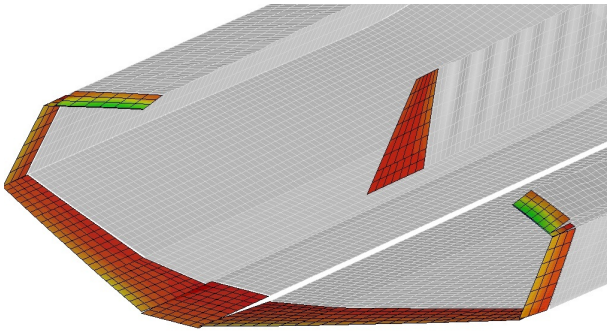


Fig. 3 Deflected Aerodynamic Grid in 1g Level Flight

method (VLM) including a Trefftz plane analysis for computing the induced drag and a skin friction and parasite drag model based on empirical methods [22]. Compressibility effects are considered using a Prandtl Glauert correction [23]. Time domain unsteady aerodynamics are computed using an implementation of the unsteady vortex lattice method (UVLM) documented in [24] or [25]. Figure 3 shows an example of the aerodynamic grid used for aerodynamic and aeroelastic computations. The influence of the fuselage, except for the contribution to the friction and parasite drag is neglected.

2.2 Structural Model

A nonlinear finite element (FE) beam structure is representing the wing, the fuselage and the vertical stabilizer. For the given design a linear model would still be in the range of good accuracy, however the nonlinear model is used to exploit the full capability of the tool. For the structural design and sizing the tool dAEDalus first introduced in [26] was further developed and extended by various features described and extensively validated in [27]. The structural model shown in Figure 4 includes gravitational acceleration (inertial relief), fuel masses, nonstructural masses of moveable surfaces and actuators, systems as well as engine thrust and mass. Sizing is performed for a 2.5g pull-up, a -1g push, a roll maneuver, a sideslip maneuver and dynamic vertical and lateral gusts. The obtained minimum required equivalent skin thickness considering the above load cases is depicted as well in Figure 4.

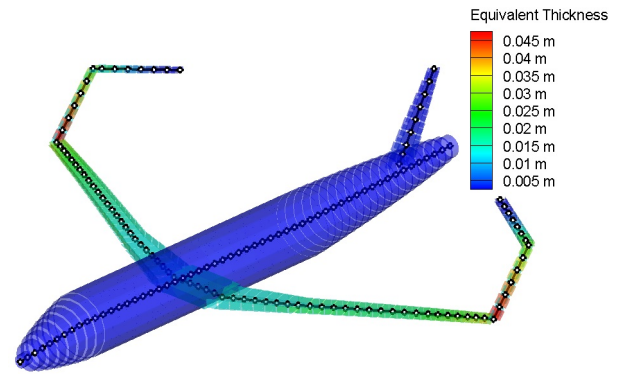


Fig. 4 Structural Beam Model

2.3 Flight Simulation

Flight simulation can be performed either by direct simulation of the tightly coupled UVLM/FE model applying the Newmark-Beta scheme for the transient FE solution or using a simplified model to achieve both real and fast time capability. The reduced order flight simulation model is automatically generated based on the previously described model and implements the rigid body nonlinear six Degrees of Freedom (6DoF) equations of motion on the center of gravity. The rigid body steady aerodynamics are computed using the VLM and are tabulated for fast interpolation during simulation. Aircraft flexibility is considered using the mean-axis approximation, well aware of the shortcomings of this method. The reduced order flexible model is obtained by transformation of the FEM model into modal coordinates using the free body modes and subsequent modal truncation [28]. The generalized aerodynamic forces (GAF) are computed using the UVLM time marching scheme about a defined reference point. The time domain unsteady aerodynamic forces are then Fourier transformed and approximated in a linear state space model using Karpel's minimum state method [29] [30]. The aeroelastic subsystem is implemented in the flight simulation as a dynamic feedback to the nonlinear rigid body equations of motion. The engines are modeled using a first order time delay, computing the thrust as a function of Mach number, altitude and thrust lever position. The atmospheric model implements the ISA atmosphere [31]. A simple landing gear model using

a damped spring-mass system for the nose gear as well as for the left and right main gear is implemented. Sensors are modeled by means of a time delay of $160ms$ and actuators apply a second order time delay. The simulation is linked to the FlightGear [32] visualization environment enabling pilot in the loop simulations. Flight Simulations can be performed under Direct law or Normal law using the control system described below.

2.4 Control System

The flight control system is designed using state of the art methods [33]. Linearized models are generated for the flight envelope shown in Figure 5 for a range of different masses, CG's, Mach numbers and dynamic pressures. A longitudinal and a lateral gain scheduled controller is designed using an automatic design algorithm described in [34]. The longitudinal control anticipation parameter (CAP) is set to 1 resulting in a closed loop short period in a range from $\omega_{sp} = 1.56rad/s$ to $\omega_{sp} = 4rad/s$. For the design of the control system, aeroelasticity is merely considered applying flex factors, hence assuming quasi steady aeroelasticity which is valid if ω_{sp} is sufficiently separated from the lowest structural modes. An integrated approach for control design such as shown by [35] is required if the rigid and elastic modes are not clearly separated.

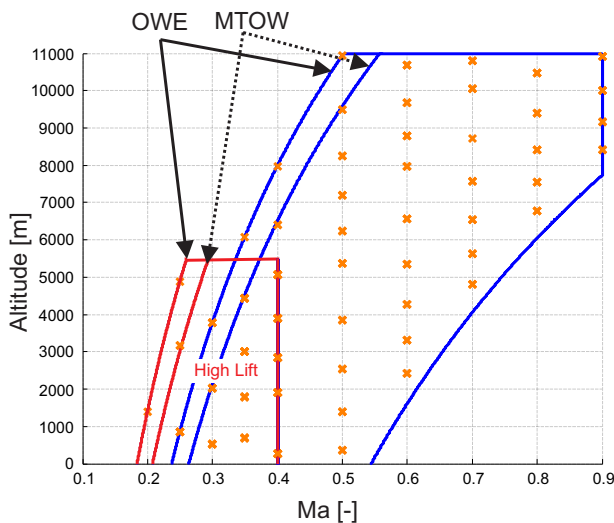


Fig. 5 Flight Envelope

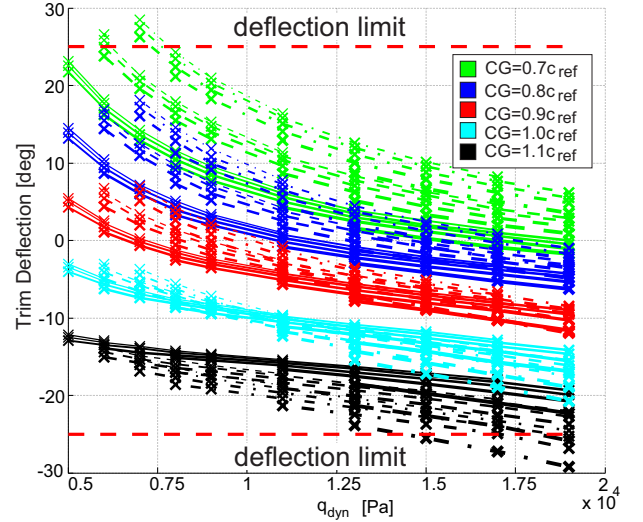


Fig. 6 C-wing Trim Deflections over Flight Envelope

3 Longitudinal Control and Stability

An important prerequisite for certification is longitudinal control and stability which will be investigated closer in this section.

3.1 Trim

For certification an aircraft needs to fulfill longitudinal trimmability [17, 1-B-19] (EASA CS-25.161) and stability [17, 1-B-20] (EASA CS-25.173) over a range of centers of gravity (CG). The required trimmable CG range is $\Delta CG = 0.32c_{ref}$ based upon experience for the given size of aircraft, where c_{ref} is the mean aerodynamic chord. Trim computations consider deformations of the aircraft structure. Figure 6 shows the required trim deflections over the flight envelope for each of the envelope points shown in Figure 5, including a variation of the aircraft mass from Maximum Take Off Weight (MTOW) to Operating Empty Weight (OEW) and a CG range of $\Delta CG = 0.4c_{ref}$. Different colors indicate the CG configuration, the line style indicates the mass, the line thickness the Mach number. Note that the two most rearward CG positions (i.e. color cyan and black) are in the statically unstable region. It can be seen that it is possible to trim the aircraft over the entire flight envelope, however not achieving the full required CG range and static stability at the same time. Further the CG must

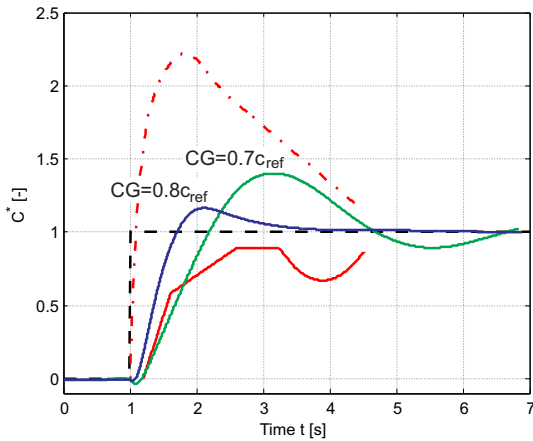


Fig. 7 Longitudinal Maneuverability Criterion [36]

be shifted from low to high speed in order to keep the required trim deflections moderate, this can be obtained by a trim tank in the rear fuselage.

3.2 Longitudinal Maneuverability

Given the reduced lever arm and the small control surface area the pitch control authority is severely reduced compared to a conventional design. The longitudinal handling quality requirement defined by [36] was evaluated in the non-linear simulation model over the flight envelope. Two examples are depicted in Figure 7, showing a low speed case for $CG = 0.7c_{ref}$ and $CG = 0.8c_{ref}$. It can be seen that the response of the more forward CG case is not within the required boundaries. It was found that the criterion for longitudinal maneuverability can only be achieved within a very limited CG and mass range for low speeds.

3.3 T/O and Landing

Take-off and landing characteristics are investigated using the fast time flight simulation model and considering high lift system aerodynamics. Takeoff simulations were performed under ISA standard conditions and an airport field height of 1487ft (MUC). A rotation speed of $V_R = 150kts$ was attempted, however a speed of $V_R = 205kts$ was required for the case with the most forward CG and MTOW. The respective takeoff trajectories are visualized in Figure 8. It can be seen that

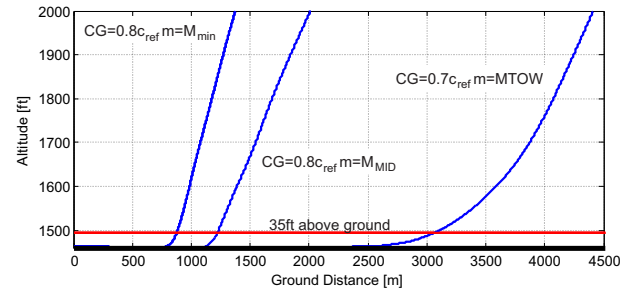


Fig. 8 Takeoff Trajectories for Different Masses and CG's

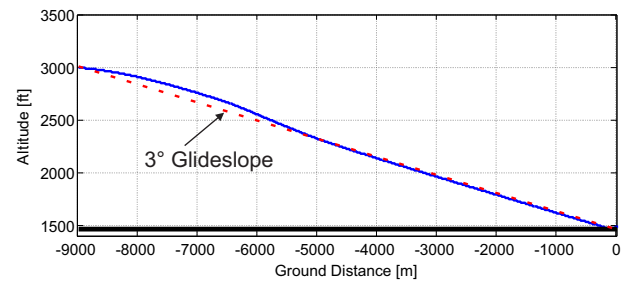


Fig. 9 Landing Trajectory

for the latter case the transition to the climb angle is too slow to ensure a safe takeoff. Furthermore the takeoff field length is exceeded by far compared to in-service aircraft with similar MTOW. Landing simulations showed similar problems due to longitudinal control authority issues. An excessive landing speed of over $200kts$ at maximum landing weight was required in order to perform a safe landing flare. Figure 9 shows a typical landing trajectory.

4 Aeroelastic Stability

Aeroelastic analysis was performed using the UVLM aerodynamics coupled to the FE structural model.

4.1 Flutter Analysis

Eigenmodes and frequencies were computed as well as the flutter speed considering different fueling cases. The eigenfrequencies of the lowest frequency modes are shown in Table 1. Figure 10 shows the three lowest eigenmodes of the C-wing.

The flutter speed was computed using a modified pk-Method presented in [37] using the linearized

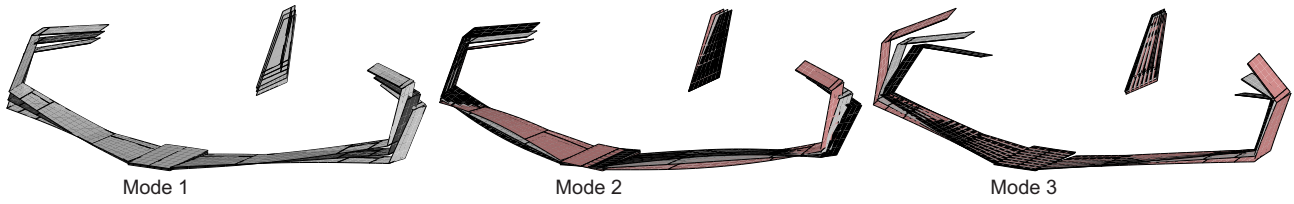


Fig. 10 Characteristic Modeshapes of the C-wing

Table 1 Eigenmode Frequencies

Mode	Fuel Empty	Fuel Full	symmetry
1	1.02Hz	0.95Hz	symmetric
2	2.17Hz	1.82Hz	antisymmetric
3	2.58Hz	2.52Hz	symmetric
4	2.61Hz	2.57Hz	antisymmetric
5	3.82Hz	3.38Hz	symmetric

model about the respective trimmed state. The result was further checked by time domain flutter analysis using the fully coupled model. An example for a root locus is shown in Figure 11 showing the first wing bending mode becoming unstable. The color shift from blue to red indicates the increase of airspeed. The flutter speed

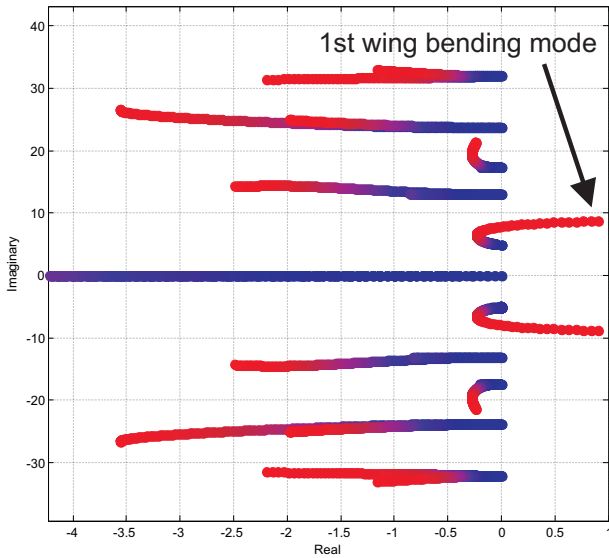


Fig. 11 Root Locus

was computed at sea level and standard ISA conditions. Flutter onset was found at $Ma = 0.88$ for the empty fuel case and at $Ma = 0.92$ with full fuel tanks. The low frequency of the wing bending mode leads to a lower flutter speed compared to a classical wing. A standard transonic

cruise speed with a safety margin of $15\%V_{EAS}$ prescribed in [17, 1-D-5] (EASA CS-25.629) can however still be achieved as shown in Figure 12.

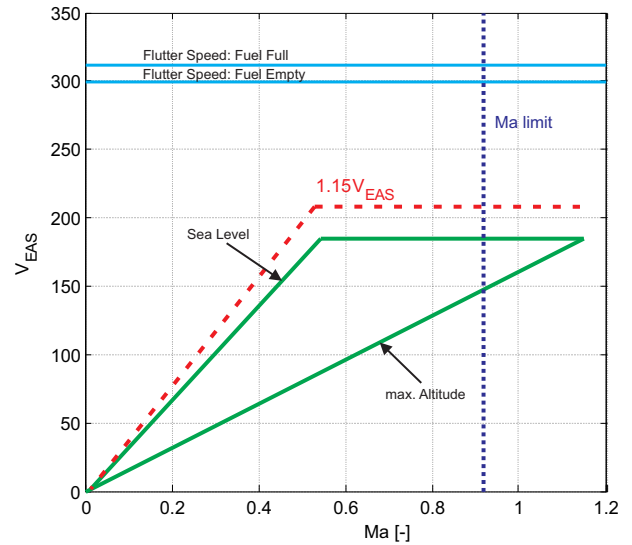


Fig. 12 Flutter Boundaries

5 Re-Design

The introduced design shows problems for essential required capabilities, therefore a re-design was conducted adding longitudinal control authority by splitting the vertical tail into a V-tail as shown in Figure 13. The V-tail is now used for pitch control and is as well used for trimming in combination with the top wing of the C-wing to achieve the minimum induced drag for a given flight state. The control surface allocation is optimized for each grid point of the flight envelope. The required trim angles are within -10° and 2° for the top wing and -12° and 8° for the V-tail. The remaining longitudinal control authority is sufficient to meet all requirements mentioned previously. The structural design is carried out using the method described for the previous design. A mass comparison is shown in Table 2,

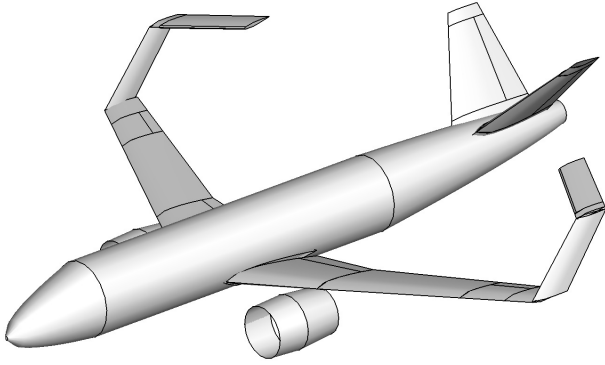


Fig. 13 Concept 2 Geometry

comparing the C-wing Concepts 1 and 2 to a design featuring a conventional wing and a V-tail. The required fuselage mass for the V-tail configuration is higher due to the additional forces acting from the tail during maneuvering. The design loads for the C-wing are however considerably lower when using the V-tail for pitch control instead of the top wing, leading to a lighter outer wing. This results in overall higher structural eigenfrequencies as shown in Table 3 and therefore had an increase of flutter speed compared to the previous design.

Table 2 Structural Masses

Mass	Concept 1	Concept 2	Conv. wing, V-tail
Payld.	20t	20t	20t
Fuel	18t	18t	18t
Fuselg.	ref	+12.5%	+11.5%
Wing	ref	-12%	-45%
Tail	ref	+143%	+160%
Total	ref	+1.2%	-2.76%

Table 3 Mode Frequencies

Mode	Fuel Empty	Fuel Full	symmetry
1	1.50Hz	1.29Hz	symmetric
2	2.26Hz	1.91Hz	antisymmetric
3	2.33Hz	2.10Hz	antisymmetric
4	2.80Hz	2.74Hz	antisymmetric
5	2.95Hz	2.89Hz	symmetric

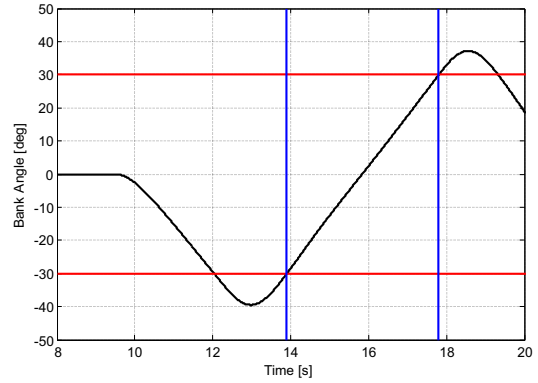


Fig. 14 Roll Control Performance

5.1 Performance

The performance of the presented concepts is compared by considering the different mass, wetted surface area and induced drag shown in Table 4. The range was computed using the Breguet equation. It was found that adding the V-Tail leads to a range loss of 8.55% for Concept 2 and 9.1% for the conventional wing configuration with V-tail when compared to Concept 1. This means that the range benefit due to induced drag reduction is largely lost due to the additional weight.

Table 4 Performance Comparison

	Concept 1	Concept 2	Conv. wing, V-tail
$C_{d,f}$	ref	+12.3%	+1.5%
$C_{d,i}$	ref	+2.3%	+32.3%
Range	ref	-8.55%	-9.1%

5.2 Lateral Control

After finding that longitudinal control requirements are achieved, lateral control is investigated. EASA CS-25.147 [17, 1-B-17] defines requirements for lateral controllability. Sufficient lateral control is shown by rolling from $\phi = -30^\circ$ to $\phi = 30^\circ$ within 7s [17, 2-B-52]. Figure 14 shows that this can be met by the presented design achieving the required change of bank angle within 3.9s. Furthermore sufficient lateral control must be guaranteed in the case of one engine

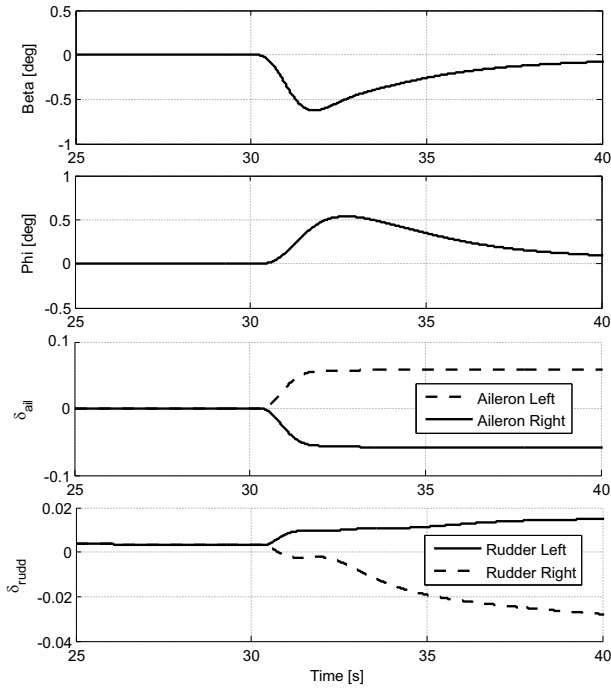


Fig. 15 Aircraft Response after OEI

being inoperative. Figure 15 shows the aircraft response after an engine failure. The engine fails at $t = 30s$, the initially caused sideslip angle is regulated to zero by a control algorithm activated upon engine failure, controlling the rudders and ailerons in order to keep the aircraft in straight flight during one engine inoperative (OEI), minimizing the pilot work load. The achieved time for the change in bank angle by $\Delta\phi = 60^\circ$ in the more critical direction is 6s as shown in Figure 16. This is longer compared to the case with both engines operative, but still meets the requirement from [17, 2-B-51] which was set at 11s.

5.3 Directional Control

In order to show sufficient lateral control the pilot must be able to safely make a reasonably sudden change in heading of up to 15 degrees. This must also be possible in case of OEI in the direction of the operative engine. The given design cannot however achieve this requirement. The V-tail causes a severe coupling of roll and yaw. The rudders cause a significant rolling moment requiring a counteraction using the ailerons. Therefore it is not considered safe to make sudden heading changes of up to 15 degrees close

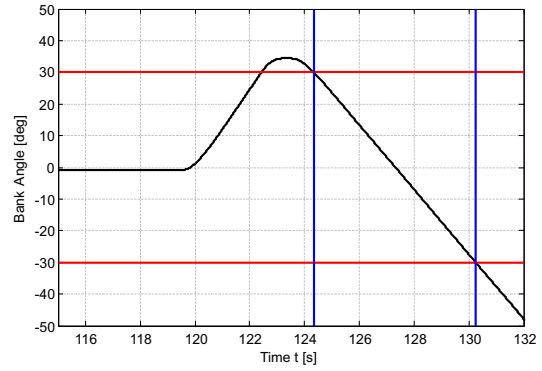


Fig. 16 Roll Control Performance OEI

to the ground. The applicability of the V-tail is therefore questionable.

6 Conclusion

The presented Airbus Group Innovations toolchain for airworthiness assessment is applied successfully to the initial and a re-design C-wing concept. After finding severe challenges for certification due to longitudinal controllability issues a re-design introducing additional longitudinal control authority is performed and further investigated. The longitudinal control requirements can be met by this re-designed concept, however new challenges arose due to the V-tail causing a heavy coupling of roll and yaw making it difficult to change the heading of the aircraft while keeping wings level. The performance of the concepts is investigated considering the different weights and drag values. It is found that the performance improvement due to drag reduction is mostly lost due to the additional weight. However a much smaller top and side wing can be designed for the C-wing if no longitudinal control authority is requested from the top wing, which was not further investigated. Although aeroelasticity was expected to be a problem, it is found that aeroelastic constraints can be met. Sizing the structure for critical loadcases provides sufficient stiffness to avoid flutter or divergence within the flight envelope and meets prescribed safety margins. All results are subject to uncertainties due to the underlying modeling theories, for details it is referred to

[27]. It must be noted that the presented designs were not optimized for performance but rather served as testcases for evaluating the presented toolchain. MDO optimization will be a topic of further research.

References

- [1] I. Kroo, "Nonplanar wing concepts for increased aircraft efficiency," *VKI lecture series on Innovative Configurations and Advanced Concepts for Future Civil Aircraft*, 2005.
- [2] D. P. Raymer, *Aircraft Design: A Conceptual Approach*. American Institute of Aeronautics and Astronautics, 2006.
- [3] E. Torenbeek, *Synthesis of Subsonic Airplane Design*. Delft: Delft University Press; Kluwer Academic Publishers, 1996.
- [4] J. Schirra and J. Watmuff, "Euler based induced drag estimation for highly nonplanar lifting systems during conceptual design," *German Congress of Aeronautical Sciences*, 2013.
- [5] J. McMasters and I. Kroo, "Advanced configurations for very large transport airplanes," in *Aerospace Sciences Meetings*, American Institute of Aeronautics and Astronautics, 1998.
- [6] A. Isikveren, A. Seitz, P. Vratny, C. Pernet, K. Plötner, and M. Hornung, "Conceptual studies of universally-electric systems architectures suitable for transport aircraft," *German Congress of Aeronautical Sciences*, 2012.
- [7] M. Trapani, M. Pleissner, A. Isikveren, and V. Wieczorek, K., "Preliminary investigation of a self-trimming non-planar wing using adaptive utilities," *German Congress of Aeronautical Sciences*, 2012.
- [8] U. Kling, C. Gologan, A. T. Isikveren, and M. Hornung, "Aeroelastic investigations of a self trimming non-planar wing," *German Congress of Aeronautical Sciences*, 2013.
- [9] A. Ning and I. Kroo, "Multidisciplinary considerations in the design of wings and wing tip devices," *Journal of Aircraft*, vol. 47, no. 2, pp. 534–543, 2010.
- [10] P. W. Jansen, R. E. Perez, and J. R. R. A. Martins, "Aerostructural optimization of nonplanar lifting surfaces," *Journal of Aircraft*, vol. 47, no. 5, pp. 1490–1503, 2010.
- [11] S. Binder, "Generation of aerodynamic and aeroelastic datasets for flight simulation on the example of a c-wing," Master's thesis, Technische Universität München, 2013.
- [12] R. C. Schwanz, "Formulation of the equations of motion of an elastic aircraft for stability and control and flight control applications," *National Technical Information Service*, 1972.
- [13] D. K. Schmidt, *Modern Flight Dynamics*. New York: McGrawHill, 2011.
- [14] I. Tuzcu, *Dynamics and Control of Flexible Aircraft*. PhD thesis, Virginia Polytechnic Institute and State University, 2001.
- [15] H. Hesse and R. Palacios, "Consistent structural linearization in flexible aircraft dynamics with large rigid-body motion," *AIAA*, 2013.
- [16] M. Drela, "Integrated simulation model for preliminary aerodynamic structural, and control-law design of aircraft," *AIAA*, pp. 1644–1656, 1999.
- [17] European Aviation Safety Agency, "Cs-25: Certification specifications and acceptable means of compliance for large aeroplanes, amendment 14," December 2013.
- [18] D. S. Soban and D. J. Biezad, "Computer optimization of aircraft handling qualities during preliminary design," *IEEE*, 1995.
- [19] R. Caja and D. Scholz, "Box wing flight dynamics in the stage of conceptual aircraft design," in *German Congress of Aeronautical Sciences*, 2012.
- [20] S. Bhasin, P. Chen, Z. Wang, and L. Demasi, "Dynamic nonlinear aeroelastic analysis of the joined wing configuration," in *Structures, Structural Dynamics, and Materials and Co-located Conferences*, American Institute of Aeronautics and Astronautics, 2012.
- [21] H. J. Damveld, *A Cybernetic Approach to Assess the Longitudinal Handling Qualities of Aeroelastic Aircraft*. PhD thesis, Technical University of Delft, 2009.
- [22] I. Kroo, *Aircraft Design: Synthesis and Analysis*. Dept. of Aero/Astro, 2010.
- [23] A. H. Shapiro, *The Dynamics and Thermodynamics of Compressible Fluid Flow*. Ronald Press, 1953.
- [24] J. Katz and A. Plotkin, *Low-Speed Aerodynamics*. Cambridge University Press, second edition ed., 2001.
- [25] J. Murua, R. Palacios, and J. M. R. Gra-

ham, “Applications of the unsteady vortex-lattice method in aircraft aeroelasticity and flight dynamics,” *Progress in Aerospace Sciences*, vol. 55, pp. 46–72, Nov 2012.

- [26] K. Seywald, “Wingbox mass prediction considering quasi steady aeroelasticity,” Master’s thesis, Technical University of Munich, 2011.
- [27] K. Seywald, N. Gomes de Paula, A. Wildschek, F. Holzapfel, M. Foerster, and C. Breitsamter, “Validation of an aeroelastic analysis and simulation tool for the assessment of innovative, highly elastic aircraft configurations,” *German Congress of Aeronautical Sciences*, 2014.
- [28] M. Karpel, “Reduced-order aeroelastic model via dynamic residualization,” *Journal of Aircraft*, 1990.
- [29] M. Karpel and E. Strul, “Minimum-state unsteady aerodynamic approximations with flexible constraints,” *Journal of Aircraft*, vol. 33, pp. 1190–1196, November-December 1996.
- [30] D. H. Baldelli and P. Chen, “Unified aeroelastic and flight dynamic formulation via rational function approximations,” *Journal of Aircraft*, vol. 43, May-June 2006.
- [31] International Organization for Standardization, “Standard atmosphere,” *ISO 2533:1975*, 1975.
- [32] A. R. Perry, “The flightgear flight simulator,” in *UseLinux*, 2004.
- [33] R. Brockhaus, *Flugregelung*. Berlin: Springer Berlin, 2010.
- [34] F. Hellmundt, “Entwurf von regelgesetzen mit gain scheduling für die robustheitsanalyse von konfigurationsmodifikationen eines flugzeugs unter berücksichtigung der erreichbaren handling qualities,” Master’s thesis, Technische University München, 2013.
- [35] M. Hanel, “Integrated flight and aeroelastic control of a flexible transport aircraft,” *AIAA*, pp. 1002–1011, 1998.
- [36] H. Tobie, E. Elliott, and L. Malcom, “A new longitudinal handling qualities criterion,” *Proceedings of the 18th National Aerospace Electronics Conference*, pp. 93–97, 1966.
- [37] R. Botez, A. Doin, and I. Cotoi, “Method for flutter aeroservoelastic open loop analysis,” *ASME 2002 International Mechanical Engineering Congress and Exposition*, 2002.

Copyright Statement

The authors confirm that they, and/or their company or organization, hold copyright on all of the original material included in this paper. The authors also confirm that they have obtained permission, from the copyright holder of any third party material included in this paper, to publish it as part of their paper. The authors confirm that they give permission, or have obtained permission from the copyright holder of this paper, for the publication and distribution of this paper as part of the ICAS 2014 proceedings or as individual off-prints from the proceedings.

7 Contact Author Email Address

klaus.seywald@airbus.com